ORIGINAL ARTICLE

lajss.org© Latin American Journal of Solids and Structures

www.lajss.org

Safety Assessment of Insensitive and Conventional Energetic Materials using 50mm Small Standard Shaped Charges: Numerical and Experimental Insights

Muhammad Saqib Awan[a], Zheng Xiang Huang[a*], Xu-dong Zu[a], Qiang Qiang Xiao[a], Ma Bin[a]

[a]School of Mechanical Engineering, Nanjing University of Science and Technology, Nanjing,210094, China. E-mails: saqib@njust.edu.cn, huangyunjust@outlook.com, zuxudong9902@njust.edu.cn, xiao_wawj@njust.edu.cn, mabin@njust.edu.cn

*Corresponding author

https://doi.org/10.1590/1679-78258054

Abstract

The detonation of conventional munitions due to accidents or hostile actions causes urban destruction and loss of life, underscoring the need for improved safety measures. This study addresses the scarcity of research in munitions safety by investigating the threat of small and medium munitions. Experimental setups using 50mm shaped charges were developed and simulated with ANSYS AUTODYN, featuring JH-2 explosive and oxygen free high conductivity copper liner. Aluminum buffer plates were added to align jet energy levels with small and medium munitions' requirements. Safety assessments of JH-2 explosive against standard charges utilized ϕ45x40mm JH-2 targets covered with steel. Numerical simulations employed the Lee-Tarver ignition and growth model, comparing JH-2 explosive response with insensitive explosives like LX-17 and TATB. Results showed JH-2's failure in experimental tests, corroborated by simulations, while TATB and LX-17 remained stable. This study advocates for the adoption of cost-effective, insensitive explosives in next generation weaponry to mitigate unintentional detonations.

Keywords

Small standard shaped charge, insensitive munitions, shaped charge jet initiation, X-ray photography; Lee-Tarver ignition and growth model, JH-2 explosive

Graphical Abstract

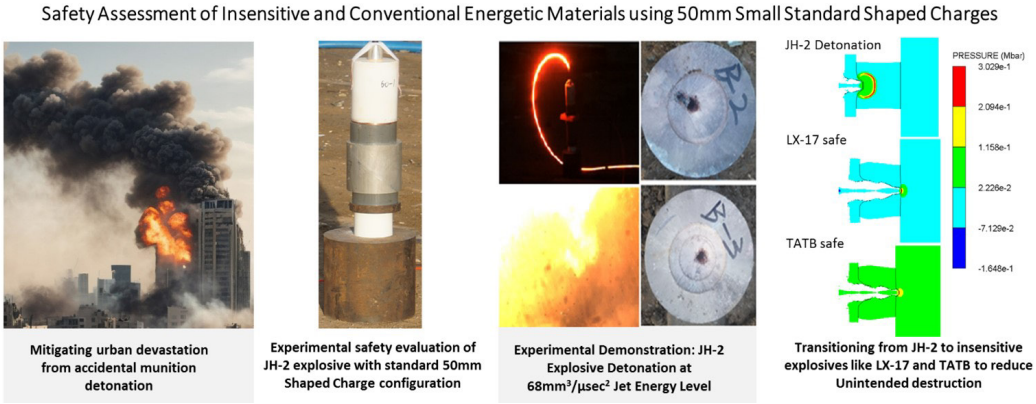

Received February 20, 2024. In revised form February 26, 2024. Accepted March 04, 2024. Available online March 13, 2024.
https://doi.org/10.1590/1679-78258054

Latin American Journal of Solids and Structures. ISSN 1679-7825. Copyright © 2024. This is an Open Access article distributed under the terms of the Creative Commons Attribution License, which permits unrestricted use, distribution, and reproduction in any medium, provided the original work is properly cited.

1 INTRODUCTION

Munitions are at risk of heat and shock threats that could occur throughout their manufacturing, transportation, storage, and operational deployment. In December 1917, a tragic incident occurred in the harbor of Halifax, Canada, where a Belgian boat collided with a French cargo ship that was carrying ammunition. The collision led to the loss of approximately 5,000 lives (Gilbert 1991). Between the years 1948 and 1994, there was an average of one occurrence every five years in the United States alone where incidents involving stored explosive materials took place. As reported by the Munitions Safety Information Analysis Center (MSIAC), there were a total of 17 incidents involving munitions worldwide during the initial half of 2004 (Hayles 2005). Separate incidents involving different aircraft carriers, resulted in the loss of 660 lives, destruction of 42 aircraft, and the approximate loss of assets worth 4 billion dollars (Davis and Louise 1989). The incident at Camp Doha had devastating consequences, as it not only resulted in the near-total loss of an entire battalion but also created a dangerous radioactive environment due to the utilization of depleted uranium in 120 mm penetrators(Scherpelz et al. 2000). Therefore, there is an urgent need to assess munitions safety against different heat and shock stimuli.

Shaped charges represent one of the most formidable shock threats encountered by munitions throughout their life cycle. Shaped charges find extensive applications in both military and civilian contexts. Shaped charges are widely employed in various military applications, encompassing land, air, and sea warfare scenarios (Shekhar 2012). Shaped charges find utilization in the destruction of tanks, bunkers, naval surface vessels, submarines, and aircraft. In civilian applications, they are employed to induce long crack formation in the oil industry (Ahmed and Malik 2017), thick or long metal structure cutting, breaking a rock (mining industry) or demolishing a concrete structure (Q. Zhang et al. 2021). Hypervelocity impact research in space also involves shaped charges (Selivanov et al. 2021). Hence, among the six assessment tests conducted on munitions, one of them is the shaped charge jet impact test. This test necessitates meeting the pass criteria of no reaction more severe than an explosion(NATO 2010). A prominent example for conducting standard shaped charge threat assessment is STANAG 4526 (STANdardization AGreement) shaped charge jet munitions test procedure. As per this agreement, a 50 mm Rockeye was utilized as the standard shaped charge. However, its performance exhibited variability, particularly concerning the Held criteria (v^2d) that determines the energy level of the jet, where the jet tip diameter is denoted by d and its tip velocity is represented by v (Arnold, W. and Rttenkoler 2012). Moreover, its test setup was not fully defined (e.g. conditioning plate, target nose, etc.) (Peron 2004). Hence, it becomes imperative to develop a standardized shaped charge for evaluating the safety of munitions.

In 2018, M. B. Brian Fuchs et al. presented an updated version of the STANAG 4526 test procedure, introducing different test procedures for small, medium, and RPG-7 level threats, which are employed globally. Additionally, they highlighted deficiencies and appropriate methodologies within this context (Fuchs 2018). Rocket-propelled grenades (RPGs) were identified as the most significant threat to munitions in recent warfare scenarios, with a v^2d value of 141 $mm^3/\mu s^2$ (Spasskiy 2001). However, numerous experts have highlighted that smaller shaped charges, such as "Top Attack Bomblets," and “40mm grenades” also pose a significant threat to the safety of munitions. E.L. Baker et al. conducted a numerical study to model surrogate representations of 40 mm grenades (Baker et al. 2015). Weaponry has been classified into four distinct categories based on their v^2d values, encompassing top-attack bomblets and extending to large anti-tank missiles(Daniels et al. 2017). It is possible to devise four distinct test configurations, however, observations indicate that only specific types of explosive initiation transpire. Nearly all of the munitions detonate, with the exception of certain highly insensitive ordnance that remains secure under the RPG7 threat level (Arnold and Rottenkolber 2013). Therefore, it is recommended to focus on utilizing only two specific types of shaped charge test setups, one representing RPG7 and higher-level threats(Baker et al. 2013), and the other representing small and medium munitions. This study aims to address this problem by proposing the use of standardized small shaped charges as representatives of small and medium-sized munitions for assessing munitions safety.

The JH-2-50 mm shaped charge was both modeled and experimentally examined as a standard representation of small and medium munitions. The JH-2 50mm shaped charges possess cone apex angles of 60 degrees. In order to adjust the V2d values of shaped charge jets, buffer plates made of aluminum and steel were utilized. v^2d value is not being used as an explosive initiation reference but only to identify munitions class. These plates had varying thicknesses, with aluminum measuring 60mm and steel measuring 10mm combined with 60mm of aluminum. A munitions safety assessment was conducted on small JH-2 targets.

2. Experimental studies of small standard shaped charge and JH 2 explosive target

2.1 Small standard shaped charge design

The investigation of jet impact performance on the JH-2 explosive entails the utilization of a 60-degree conical liner shaped charge. The dimensions and visual depiction of the shaped charge, encompassing a detonator, JH-2 explosive and metal liner, are demonstrated in FIGURE 1(a) and 1(b). The choice of copper OFHC as the liner material stems from its exceptional penetration capabilities. Upon initiation by the detonator, spherical detonation waves disperse outward from the ignition point. These waves propagate at the explosive detonation velocity, estimated at approximately 8 km/sec in this specific case, under the influence of the Chapman-Jouguet detonation pressure. Subsequently, the liner material converges along the centerline following the onset of the detonation shock wave. Ultimately, the shaped charge yields an intense jet of high-speed liner material.

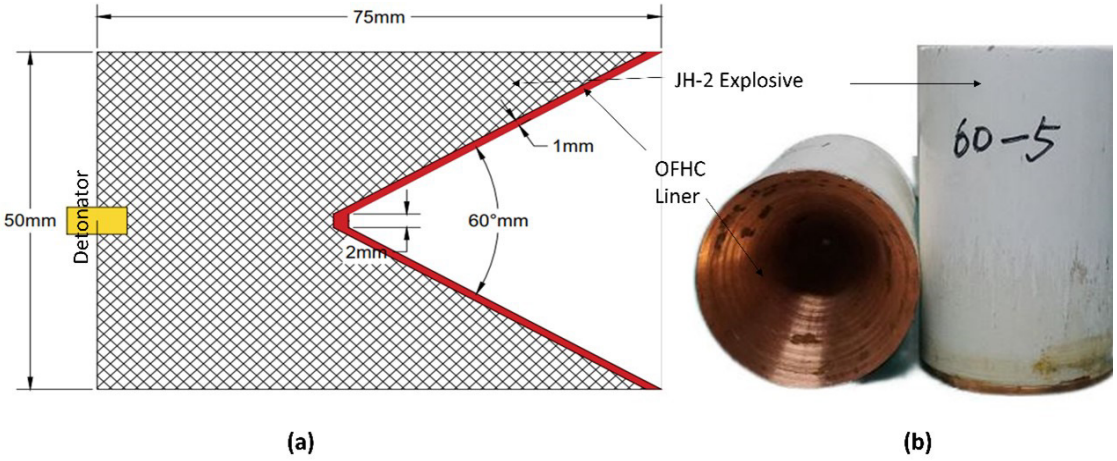

Fig. 1 50mm JH-2 shaped charge dimensions (a) and image (b)

2.2 Test Setup for Safety Assessment of JH-2 Explosive

The performance of the shaped charge was modified in accordance with small and medium munitions using two different buffer plate configurations. First configuration involved a 60mm aluminum plate and second consisted of a combination of 10mm steel and 60mm aluminum plates. The experimental setup included the shaped charge, buffer plates, a steel base cylinder, a standoff cylinder, and the JH-2(70RDX/30TNT) explosive target (Xiao et al. 2016). Figure 2 provides a visual representation of the buffer plates, steel base cylinder, standoff cylinder, and the JH-2 explosive used in the experiments. JH-2, also known as 8701 explosive, has Chapman-Jouguet pressure and performance similar to COMPB conventional explosive. Consequently, it was chosen as the target explosive for this study. The target JH-2 explosive had dimensions of 45mm in diameter and 40mm in height.

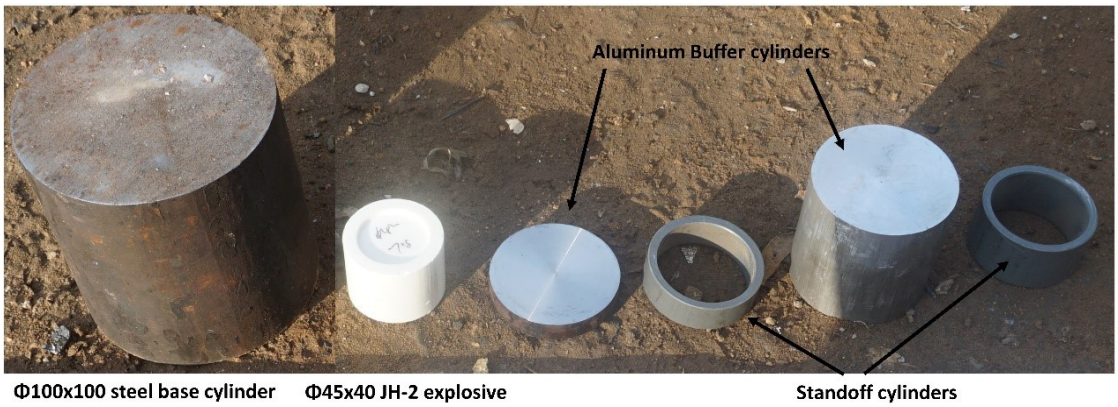

Fig. 2 Different elements of standard shaped charge test configuration

2.3 Safety assessment set up configurations

Four different configurations were employed to evaluate the JH-2 explosive's response against the standard shaped charge. Configuration one setup consisted of a shaped charge, a 25mm standoff distance between the shaped charge and a 60mm aluminum buffer plate, and a JH-2 explosive target covered with a 10mm steel plate placed at a distance of 15mm from the aluminum buffer plate as listed in table 1 along with other 3 configurations. Figure 3 also provides a general pictorial overview of first two configurations.

Table 1. Safety assessment configurations utilized for experimental and numerical evaluation of JH-2 explosive safety

Configuration	Shaped Charge	Standoff(mm)	Buffer Plate Thickness(mm)	Standoff(mm)	Explosive Cover	Target
1	50mm SC	25	60 Aluminum	15	10mm	JH-2
2	50mm SC	25	60 Aluminum	15	20mm	JH-2
3	50mm SC	25	10 Steel/60 Aluminum	5	10mm	JH-2
4	50mm SC	25	10 Steel/ 60 Aluminum	5	20mm	JH-2

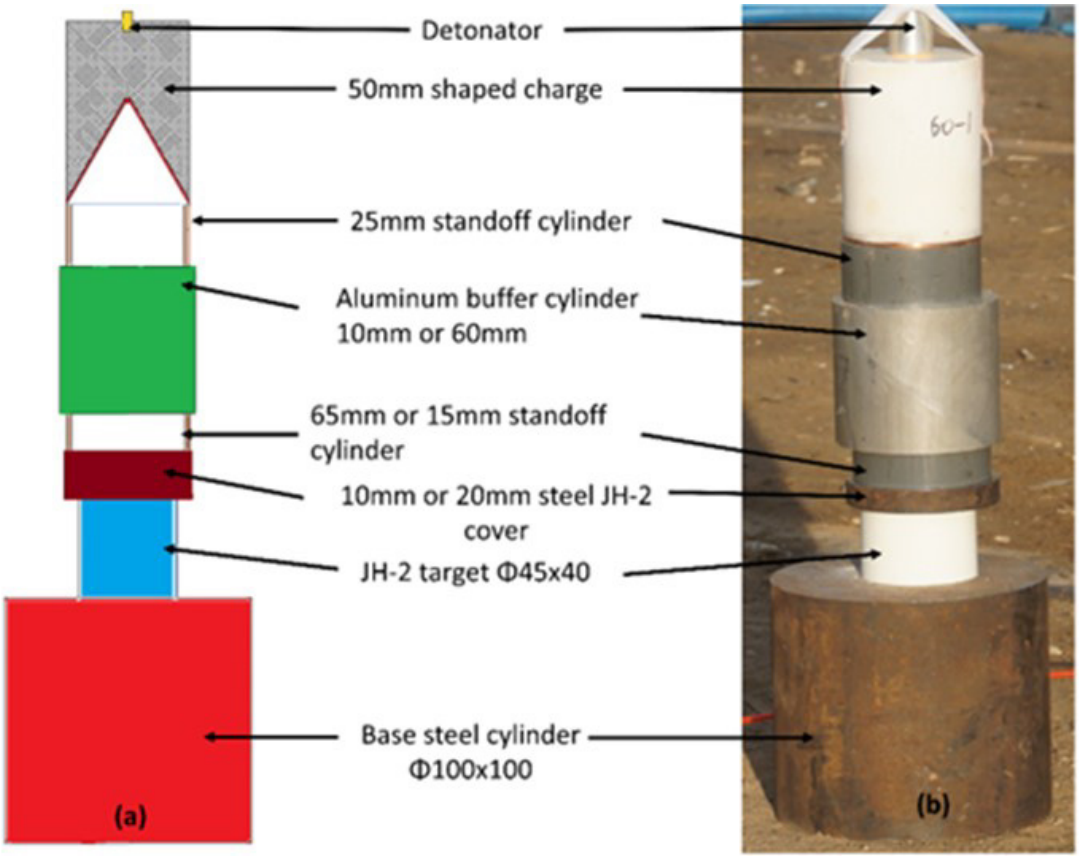

Fig. 3 JH-2 explosive safety assessment setup schematic design (a) and real image (b)

2.4 Flash X-ray set up

The experimental setup is described in Figure, providing a visual representation of the apparatus used in the study. To accurately observe and measure the jet tip diameter and its velocity, flash X-ray technology was employed. This method enables the capture of instantaneous images during the collapse of the metallic liner into a jet. Upon initiation of the shaped charge, copper metallic jet is created rapidly at high velocity, reaching speeds of several kilometers per second. By employing two X-ray tubes that emit X-rays at different time delays, two distinct moments in the jet evolution can be captured, allowing for detailed observations of the jet's morphology and position. By applying the geometric

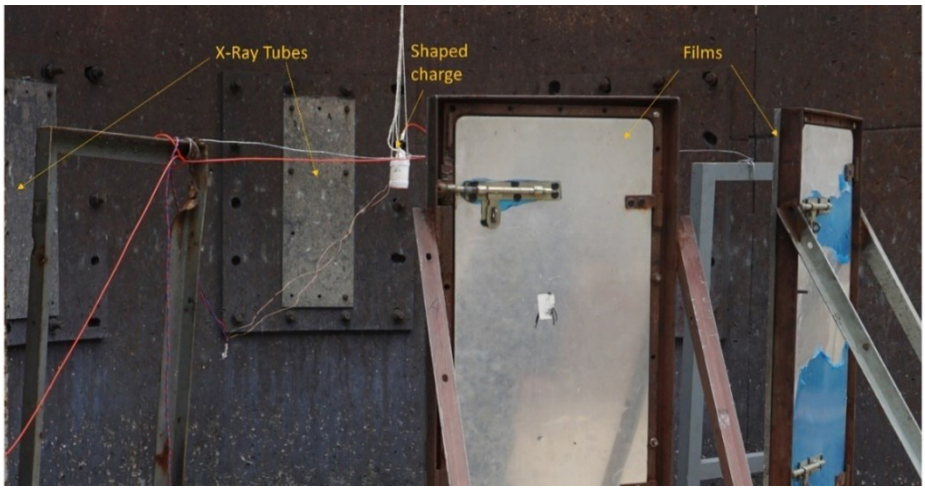

Fig. 4 Flash X-ray setup to gauge diameter and velocity of the shaped charge

similarity principle, critical jet characteristics, including length, diameter, and average velocity, can be determined. This methodology facilitates a comprehensive analysis of the shaped charge jet's behavior during the experimental investigations as depicted in figure 4.

2.5 Steel base cylinder baseline/penetration test

To compare the effects of detonation on the steel cylinder with the normal shaped charge jet penetration behavior, a baseline penetration test was conducted. The Shaped charge penetration ability was measured on 45-steel target. The densities of this specimen were 7.85 grams/cm^3 and its diameter was 100 millimeters and height was 250 millimeters as represented in figure 5.

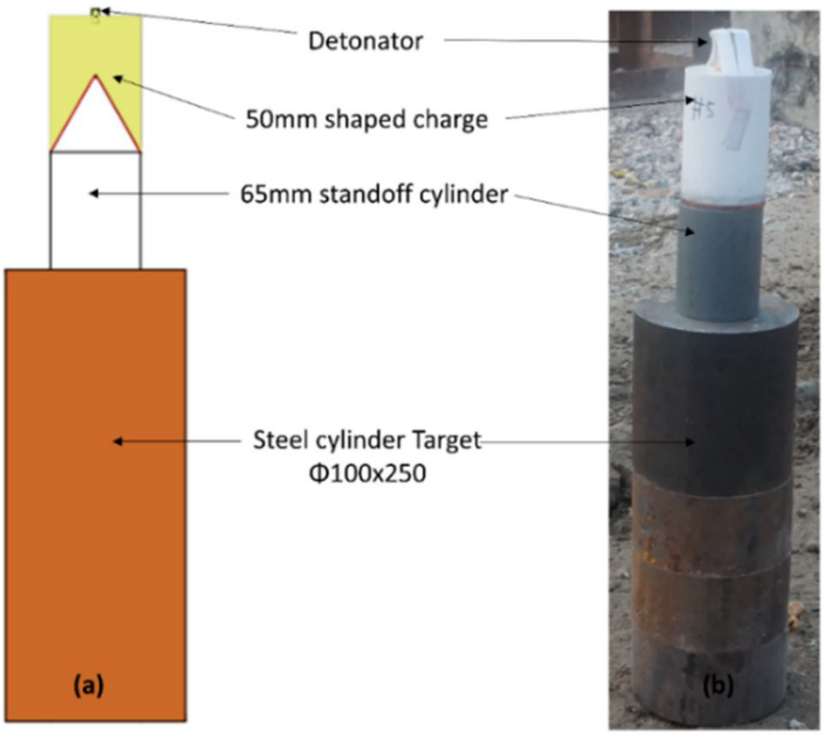

Fig. 5 Depth of penetration experiment schematic design(a) and real image(b)

3. Experimental results and analysis

3.1. Flash X-ray results

A flash X-ray study revealed a 6.13km/sec velocity and 3mm diameter for shaped charges. Numerical simulations confirmed these findings as well as depicted in figure 6(b). Moreover, the velocity of the shaped charge jet varies linearly over its length. To avoid over-statement of the v^2d values, shaped charge jet diameter and velocity should be measured behind jet tip anomalies as shown in figure 6(a).

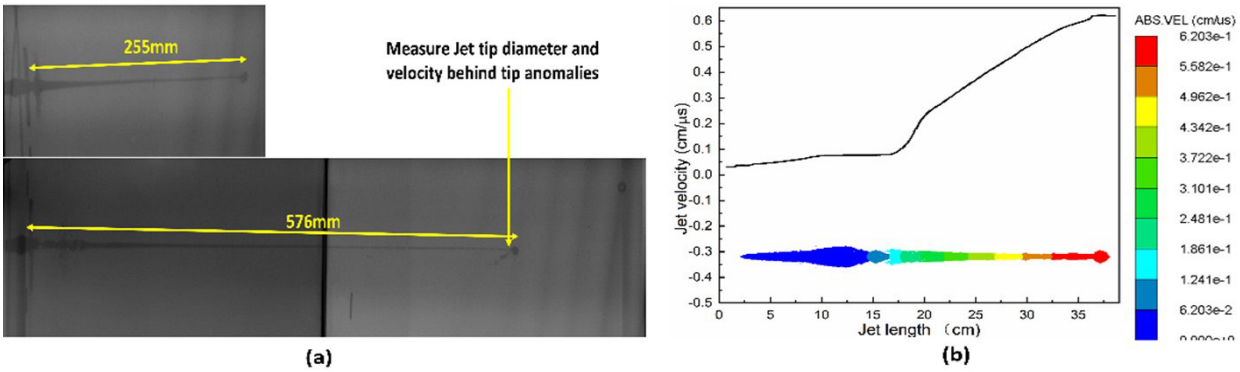

Fig. 6 (a) Flash X-ray images of the jet at 26 and 55μsec. (b) simulated velocity distribution within a shaped charge jet at 35 μsec.

3.2 Damage analysis of the target

In all of the conducted experiments, the JH-2 explosive target with a diameter of 45mm and a mass of 80 grams was detonated. The JH-2 target was subjected to three different conditions: being covered with either a 10mm and 20mm steel plate for v^2d value of 37 and a 20mm steel plate for v^2d value of 68 $mm^3/\mu sec^2$ respectively. These experiments were conducted to evaluate the impact of a jet attack with energy levels equivalent to those of a 40mm grenade and medium-sized munitions on JH-2 explosive target. The results obtained from the high-speed camera recordings clearly demonstrate that the explosive material was instantaneously consumed by detonation, as observed in the figures 7, 8, and 9. It was only covered from top and bottom with a 10,20mm steel top cover and a ϕ100x100mm steel bottom cylinder. Full encasement of the explosive material from all sides was deliberately avoided, as it would lead to enhanced confinement, thereby elevating the probability of detonation. In addition, there is another proof that the detonation occurred by virtue of the full consumption of the JH-2 target explosive.

Fig. 7 High speed camera shows detonation of JH-2 target explosive covered with 20mm casing with input v^2d value of $68mm^3/\mu sec^2$.

Fig. 8 High speed camera shows detonation of JH-2 target explosive covered with 10mm casing with input v^2d value of $68mm^3/\mu sec^2$.

Fig. 9 A high-speed camera records JH-2 explosive detonation using buffer plates (10mm steel, 60mm aluminum), replicating a 40mm grenade's performance against 10mm steel cover for JH-2 explosive.

3.3 The damage to steel base cylinder

Standard shaped charges easily penetrated the steel and aluminum buffer plates of various thicknesses and went on to strike the target with enough energy to cause detonation of JH-2 explosive. Further evidence of detonation of target explosive is crater on steel base cylinder figures 10 (a), (b) and (c) as compared with normal penetration experiment performed on the explosive as shown in figure 10 (d). This phenomenon is due to the impact of detonation shock waves on steel base cylinder, and it can also be observed in AUTODYN simulations as shown in figure 14(c), while in the absence of detonation shock wave no crater exists in AUTODYN simulation figure 15(b).

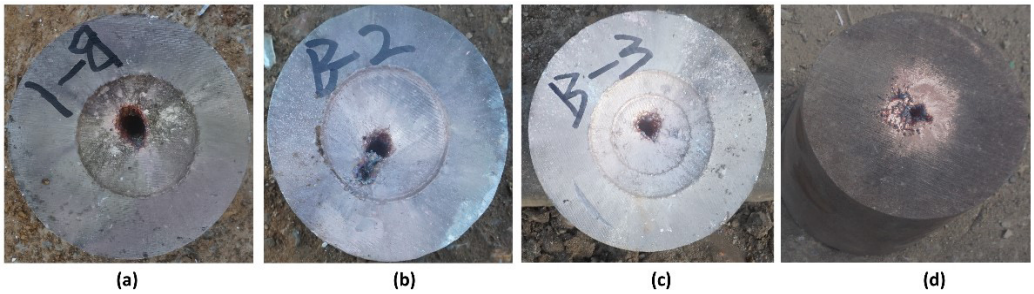

Fig. 10 (a), (b), and (c) display a crater on the steel base cylinder front side, evidencing detonation for first three configurations listed in table 1, in contrast absence of crater is evidence of no detonation in case of configuration 4.

3.4 Depth of penetration Experiment results

This test was conducted to observe the difference between normal jet interaction with steel cylinder and detonation of JH-2 explosive target on steel cylinder as shown in figure 10 (a), (b) and (c). Further, the results of penetration experiments indicate that jet penetrated roughly 230mm into the steel target shown in figure 11.

Fig. 11 Penetration behavior of shaped charge jet into steel targe (a) diameter (b) depth of penetration

4. Numerical simulation

4.1 Modeling

The nonlinear dynamics software ANSYS Autodyn was employed to conduct simulations of Shaped Charge Jet (SCJ) attacks on JH-2 explosives. In order to assess the distinctive initiation behavior of JH-2 compared to other insensitive munitions, simulations were also performed on TATB and LX-17 explosives under similar conditions. The simulation process incorporated the utilization of the Lee-Tarver ignition and growth model ,abbreviated as IGM here, IGM is known to be suitable for modeling shaped charge jet impacts that induce overdriven shocks capable of initiating explosives(X. Zhang, Huang, and Qiao 2011)(Liu, Yin, and Wang 2019). Due to the fact that some parameters of this model only fit in the unit system (cm, g, μs), AUTODYN simulations were conducted using the (cm, g, μs) units.

The simulation of the jet formation process was conducted utilizing the Euler multi-material solver, where the explosive and liner were modeled within the Euler grid. To prevent the undesired reflections during the propagation of shock waves, flow out boundaries were implemented at the ends of the computational grid which had a unit cell of 20x20cm (Elshenawy and Li 2013). The modeling scenario encompassed free space filled with air, with an assigned internal energy and density of 2.06640×10^5 and 0.001225 mg/mm^3, respectively. To measure the jet velocity, fixed gauge points were strategically positioned along the axis of symmetry. These gauge points served as reference locations for determining the velocity of the jet tip over time. To ensure the stability of the simulation results, AUTODYN's Lagrange solver was employed for simulating the penetration of the jets into the buffer plates(Li, Yang, and Lv 2014). Additionally, the erosion option in AUTODYN was utilized to maintain a reasonable time step and prevent degeneracy problems caused by excessively distorted elements in the simulation. This numerical approach helps eliminate distorted elements and ensures the integrity and accuracy of the simulation process (AUTODYN, 1998).

4.2 Constitutive equations and related parameters

The JH-2 explosive, used in both standard shaped charges and targets, was simulated using the high explosive burn modeling procedure and the Jones-Wilkins-Lee equation of state (Downes, Bouamoul, and Ensan 2014). According to Lee et al., JWL EOS takes the form given in equation 1 (E L Lee, Hornig, and Kury 1968).

$$P = A\left(1 - \frac{\omega}{R_1}\right)e^{-R_1 V} + B\left(1 - \frac{\omega}{R_2 V}\right)e^{-R_2 V} + \frac{\omega E}{V} \tag{1}$$

Where P represents pressure and R_1, A, R_2, ω, and B denote coefficients of equations 1, whereas energy is represented by E and V characterizes relative volume. These coefficients for JH-2 explosive are provided in table 2 along with D denoting the Chapman-Jouguet detonation velocity of JH-2 explosive.

Table 2. JH-2 explosive JWL equation of state parameters

D (m/sec)	ω	B (GPa)	R_1	R_2	A (GPa)	Density (g/cm^3)
8350	0.38	6.9	4.3	0.87	6.184	1.72

The detonation process of explosives under shaped-charge jet attacks was studied using IGM simulations. For explosives and detonation products, this model incorporates the Jones-Wilkins-Lee equation of state(Lee and Tarver 1980). Moreover, this model contains ignition and growth terms. As its name implies the ignition term is a mathematical depiction of hotspots forming process and consequent ignition of these hotspots. Initially, the reaction is slow to develop because isolated hotspots are burned, represented by the first growth term. Once the hotspots have begun to coalesce, the second growth term accounts for the rapid completion of the reaction(Souers, Garza, and Vitello 2002). A mathematical formulation of the Lee-Tarver IGM is given in equation 2.

$$\frac{dF}{dt} = I(1-F)^b(\eta_s - 1 - a)^x + G_1(1-F)^c\alpha^d P^y + G_2(1-F)^e\alpha^g P^z \quad (2)$$

η_s denotes the unreacted explosive's relative density and it is equal to ρ_s/ρ_o, with ρ_s being the density of remaining solid explosive and ρ_o being density when explosive was first ignited. Explosive's pressure is referred to as P, and its mass fraction is referred to as F in equation 2. And z, g, e, G_1, G_2, a, b, x, c, d, y, and I remain constant. In order to start ignition and therefore reaction, there is a critical compression parameter "a" that specifies the maximum compression which must be achieved before starting ignition and reaction. Reaction only starts when $\eta_s \geq 1+a$.

Table 3. Reaction rate parameters for Lee-Tarver model

Parameters	JH-2	TATB	LX-17	Parameters	JH-2	TATB	LX-17
I	14	$4x10^7$	$4x10^6$	d	0	$6.67\ x10^{-1}$	$`1.11\ x10^{-1}$
b	$6.67x10^{-1}$	$6.67x10^{-1}$	$6.67x10^{-1}$	y	0	4.0	1.0
a	0	$2.3x10^{-1}$	$2.2\ x10^{-1}$	G_2	40	400	400
x	4.0	7.0	7.0	e	$2.22\ x10^{-1}$	$3.33\ x10^{-1}$	$3.33\ x10^{-1}$
G_1	488	$6.3x10^4$	$6\ x10^{-1}$	g	0.666	1	1
c	$6.67x10^{-1}$	$6.67x10^{-1}$	$6.67x10^{-1}$	z	1.2	3.0	3.0

Based on the examination of the parameter values of the Lee-Tarver IGM for a wide variety of explosives, one can easily see that for most of the heterogeneous explosives, the exponents a, b, c, d, e and z remain fixed in values, which is due to the fact that they are primarily associated with the geometry of the hotspots. However, parameters I and x vary from explosive to explosive and depend on shock intensity and duration. In addition, there are four growth parameters that vary as well with changing explosive, these are G_1, y, G_2, and z. Lee-Tarver equation reaction rate parameters are given in table 3, whereas JWL parameters for reacted and unreacted parts can be found in the AUTODYN material library and the Y Liu et al paper (Liu et al. 2020).

A shock equation of state (EOS) is used to numerically represent steel target, aluminum buffer plate, and copper liner while material strength effects are depicted by the Johnson-Cook strength model. Shock-EOS describes internal energy and pressure outside and within Hugoniot curves.

$$P = P_H + \rho\Gamma(e - e_H) \quad (3)$$

There are three factors involved in Hugoniot curve analysis, Hugoniot-curve pressure P_H, material density ρ and Gruneisen coefficient Γ. e_H is Hugoniot curve energy. Johnson-Cook strength model relates yield stress, thermal softening and strain rate as follows.

$$\sigma_y = (A + B\varepsilon_p^n)(1 + Clog\varepsilon_p^*)(1 - T_H^m) \quad (4)$$

Table 4. Johnson Cook parameters for different metals used in simulation

Metal	ρ(g/cm³)	Γ	n	m	C	G(GPa)	B(GPa)	A(GPa)	T_m(K)
Aluminum	2.70	1.97	0.27	1.00	0.01	27.1	0.292	0.04	1220
Steel 45	7.83	2.17	0.26	1.03	0.014	81.8	0.51	0.792	1793
Copper	8.96	2.00	0.31	1.09	0.025	46	0.292	0.09	1356

ε^*_p is normalized plastic strain rate, while σ_y describes the dynamic behavior of yield stress and ε_p denotes effective plastic strain. In addition to these terms static yield stress is A, hardening constant is B and C is the strain rate constant in equation 4. While, m and n are thermal softening and hardening exponents respectively. Relative melting temperature is represented by T^H_m and G is shear modulus in table 4 along with other related parameters of strength model (Xu, Wang, and Chen 2019).

4.3 Modeling results

The v^2d value of the simulated 3 configurations and experimental setups is provided in figure 12. Figure 13(a), 13(b) and 13(c) illustrate the phenomenon of shaped charge jet im-pact on JH-2 explosive covered with 10mm steel casing from one side and thick steel cylinder from the other side. The shot line of jet was selected so that it passes through longest path in the explosive. The V^2d value of the impacting shaped charge jet was around 68 $mm^3/\mu sec^2$. Round parts of the JH-2 explosive did not have any kind of cover. It can be seen clearly that JH-2 explosive goes under prompt detonation (with run distance to detonation ≤10 mm) while in case of LX-17 and TATB explosive the target did not undergo any kind of full or partial detonation of explosives as no detonation shock wave can be seen in these explosives clearly depicted figure 13 (d, e, f, g, h and i).

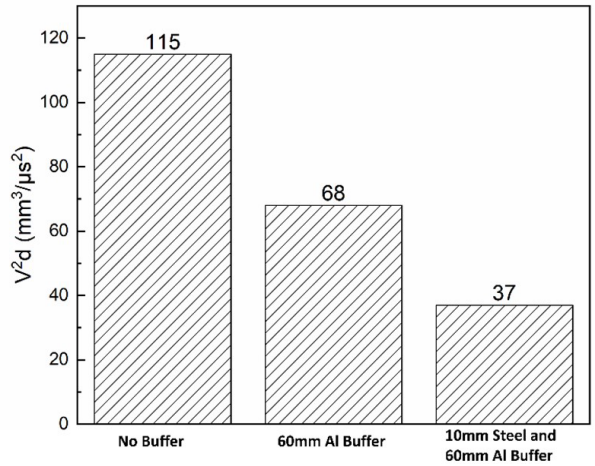

Fig. 12 Shaped charge jet energy levels with respect to buffer plates

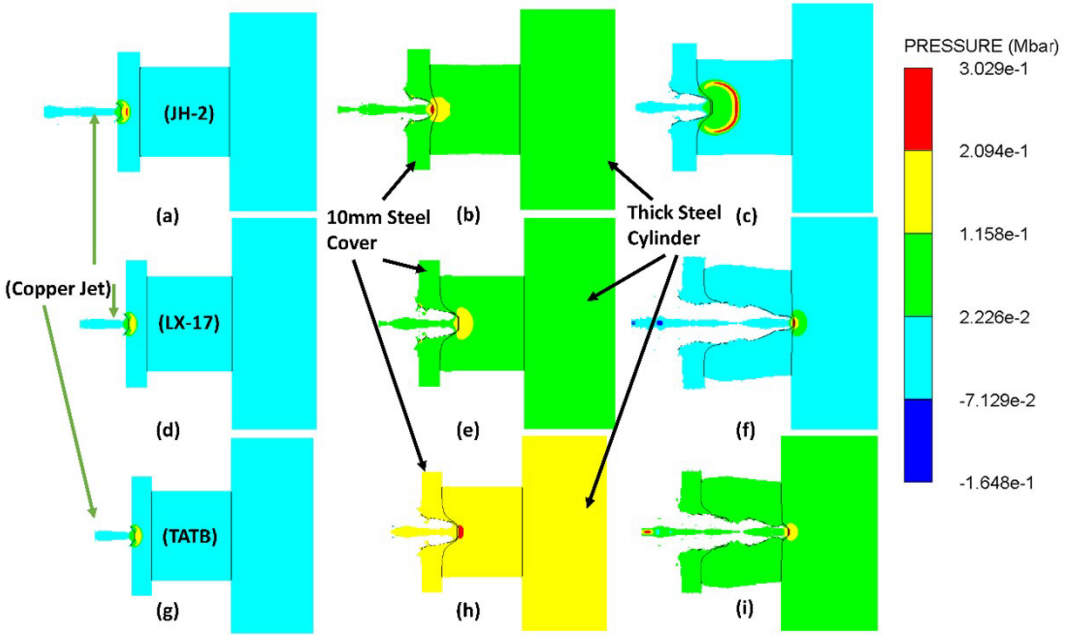

Fig. 13 Using a v^2d value of 68$mm^3/\mu sec^2$, a shaped charge jet hits 10mm steel-covered JH-2, LX-17, and TATB explosive targets. Among them, only the JH-2 explosive undergoes detonation, evident from the contour in the image.

Table 5. A total of 14 cases were simulated including three experimental configurations

Simulated cases	Explosive	Casing	v^2d ($mm^3/\mu sec^2$)	Result
1	JH-2	10 Front, 100 back	37	Fail
2	JH-2	10 Front, 100 back	68	Fail
3	JH-2	20 Front, 100 back	37	Fail
4	JH-2	20 Front, 100 back	68	Fail
5	LX-17	10 Front, 100 back	37	Pass
6	LX-17	20 Front, 100 back	37	Pass
7	TATB	10 Front, 100 back	37	Pass
8	TATB	20 Front, 100 back	37	Pass
9	LX-17	10 Front, 100 back	68	Pass
10	LX-17	20 Front, 100 back	68	Pass
11	TATB	10 Front, 100 back	68	Pass
12	TATB	20 Front, 100 back	68	Pass
13	JH-2	20 Front, 20 back	37	Pass
14	JH-2	20 All sides	37	Fail

Table 5 provides a summary of 14 simulated cases “fail” result indicates the detonation of explosive while “pass” result accounts for no detonation in explosive material. While some important explosive responses are shown in figures 13, 14 and 15. A relatively interesting shaped charge jet initiation mechanism was observed when the front steel cover thickness was increased from 10mm to 20mm and v^2d value was set at 37 $mm^3/\mu sec^2$. There was no prompt detonation. The shaped charge jet managed to pierce through the JH-2 explosive material until it approached the rear cover of the JH-2 explosive. This situation led to a substantial containment of the explosive substance between the impacting shaped charge jet and the steel base cylinder located at the back. As a consequence, an explosive shock wave was initiated, propagating in the opposite direction to the impacting jet, as illustrated in figure 14(c). This phenomenon occurs due to the steel base cylinder's ability to reflect shock waves, thereby intensifying the compression of the JH-2 explosive that was situated between the shaped charge jet and the steel base cylinder. This increased compression creates localized regions of high temperature, ultimately causing the detonation of the JH-2 explosive material.

Notably, the insensitive explosives TATB and JH-2, which were safely contained within a 10 mm casing, did not experience any form of detonation in this particular scenario as well. This outcome can be attributed to the fact that the shock waves reflected by the steel base were insufficient to generate the necessary hotspots within these less sensitive explosive materials. Another what if scenario involved a relatively thin back casing of 20mm resulted in no detonation of JH-2 explosive as presented in figure 15(b). While, munitions are mostly covered from all sides so this scenario was also simulated and resulted in the penetrative detonation of JH-2 explosive near the side casing as shown in figure 15 (c).

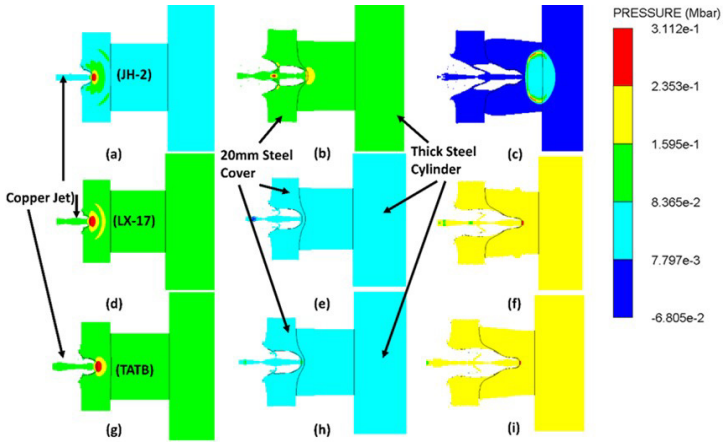

Fig. 14 In the 20mm casing, strong confinement between shaped charge jet and steel base causes detonation in JH-2 explosive, moving opposite to the jet. LX-17, TATB remain safe.

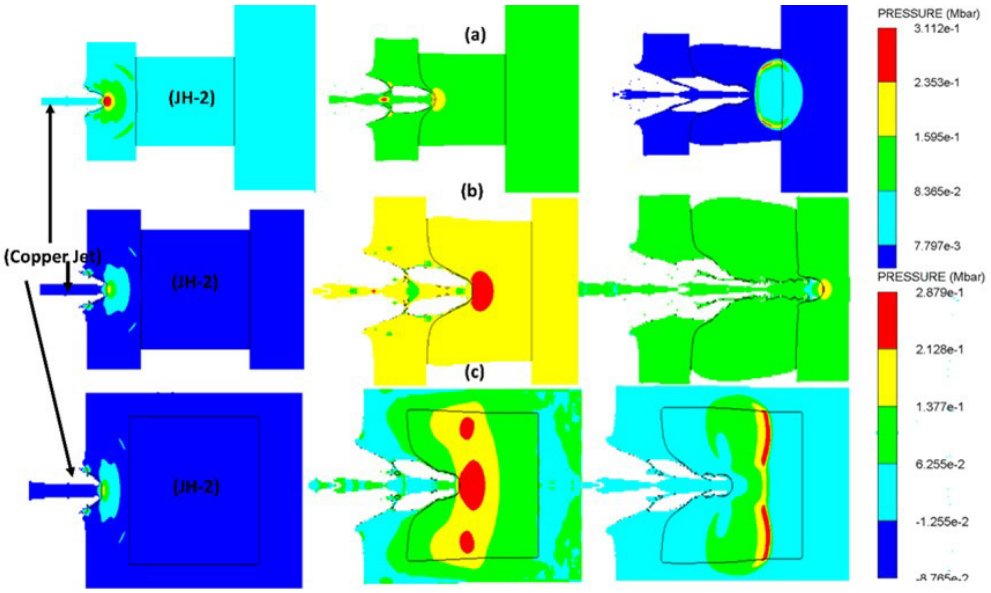

Fig. 15 Confinement impact on JH-2 explosive detonation: (a) Robust 100mm steel casing and (c) full confinement of explosive from all sides generate high-pressure hot spot from reflected shock, leading to detonation. (b) Thin 20mm steel casing lacks strong shock reflection, preventing detonation.

The gauge point pressure profile depicted in figure 16 provides numerical evidence of JH-2 explosive detonation. As the shaped charge jet penetrates, the pressure within the explosive steadily increases due to the formation of hotspots resulting from the compression caused by the impinging jet. This continuous hotspot generation elevates the internal pressure until it reaches the detonation threshold, represented by the Chapman-Jouguet pressure of approximately 0.3 Mbar for JH-2 explosive. In contrast, for LX-17 and TATB explosives, the pressure within remains consistently below their respective Chapman-Jouguet pressures, as shown in figures 17 and 18. This is attributed to less efficient hotspot generation compared to conventional JH-2 explosive. As a result, these insensitive explosives remain unaffected by the shaped charge jet with energy levels equivalent to medium munitions in all three cases.

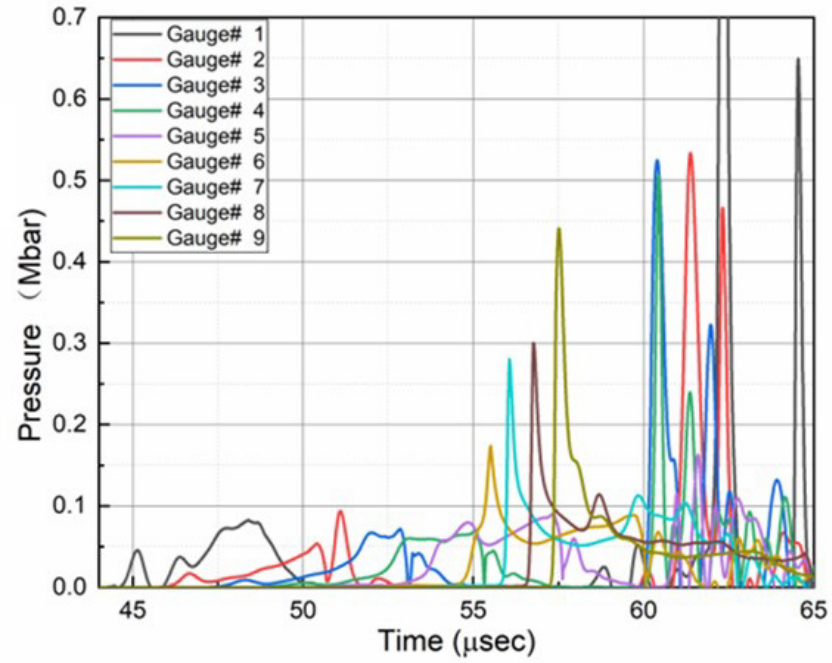

Fig. 16 Gauge points inside the explosive, spaced 5 mm apart, show pressure rising until Chapman-Jouguet pressure approximately 0.3 Mbar is reached, causing detonation in JH-2 explosive

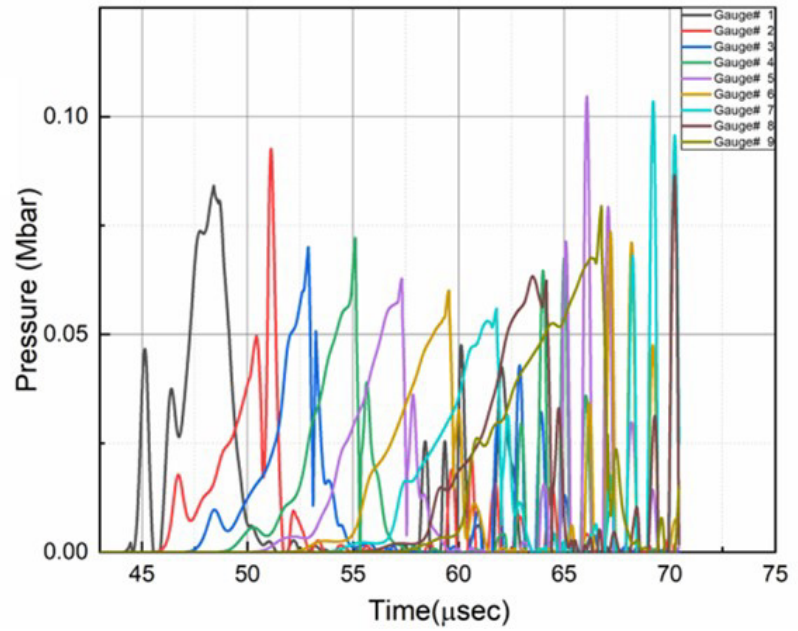

Fig. 17 Gauge points within the explosive, placed every 5 mm, reveal no detonation; pressure stays significantly under LX-17's Chapman-Jouguet threshold pressure for detonation.

The gauge point pressure profile depicted in figure 16 provides numerical evidence of JH-2 explosive detonation. As the shaped charge jet penetrates, the pressure within the explosive steadily increases due to the formation of hotspots resulting from the compression caused by the impinging jet. This continuous hotspot generation elevates the internal pressure until it reaches the detonation threshold, represented by the Chapman-Jouguet pressure of approximately 0.3 Mbar for JH-2 explosive. In contrast, for LX-17 and TATB explosives, the pressure within remains consistently below their respective Chapman-Jouguet pressures, as shown in figures 17 and 18. This is attributed to less hotspot generation compared to conventional JH-2 explosive. As a result, these insensitive explosives remain unaffected by the shaped charge jet with energy levels equivalent to 40mm grenade in all three cases The agreement between the experimental outcomes and the simulations of penetration depth is notable. The numerical calculation of penetration depth, as depicted in figure 19, is approximately 233mm.

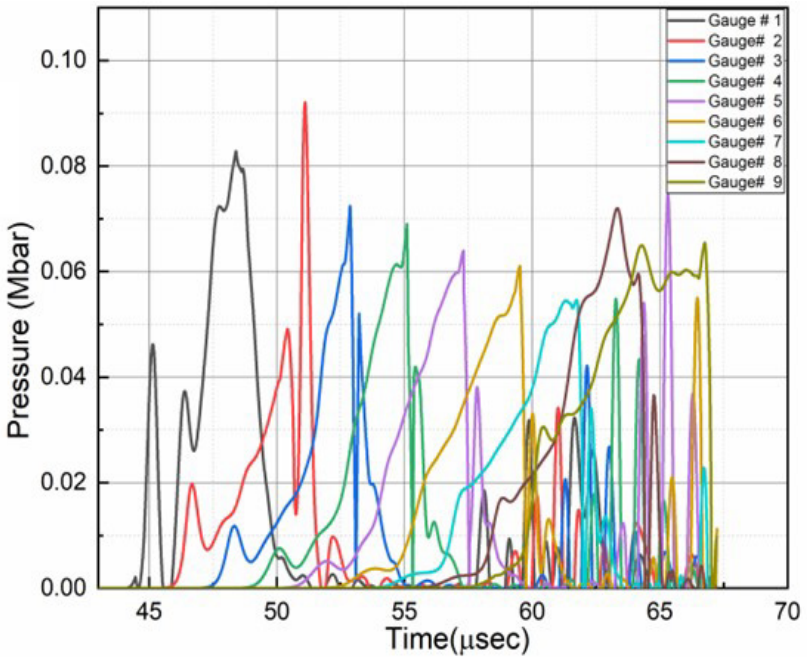

Fig. 18 Gauge points within the explosive, spaced every 5 mm, demonstrate absence of detonation; pressure stays notably below TATB's Chapman-Jouguet threshold pressure for detonation.

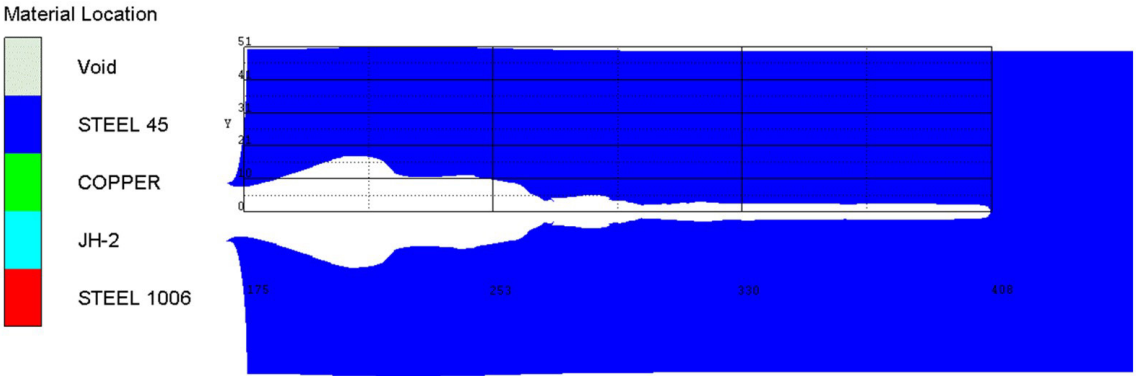

Fig. 19 The numerical prediction indicates a penetration depth of around 233mm, a close match to the experimental measurement of 230mm at a stand of distance 2 times the shaped charge diameter.

5. Discussion

The phenomenon of explosive initiation by a shaped charge jet is a well-researched topic and has provided evidence of the detonation of conventional munitions, such as TNT and COMPB explosives, under the attack of a shaped charge jet (Held 1987). However, safety analysis studies, standard tools for the safety analysis of munitions against shaped charge jet attack, and preventive measures have been sparsely studied. This paper aims to fulfill that gap by providing standard safety assessment tools that represent small munitions with v^2d values in the range of 60-70 $mm^3/\mu sec^2$, as well as 40mm grenades with a v^2d value of approximately 40 $mm^3/\mu sec^2$. It also offers an experimental and numerical analysis of the response of the conventional JH-2 with respect to munition safety.The detonation of the JH-2 target explosive was observed at 68 $mm^3/\mu sec^2$ for both 10mm and 20mm steel covers, as well as at 37 $mm^3/\mu sec^2$ in the case of a 10mm steel cover. This underscores the critical need to explore alternative, safer explosive compounds. We suggest replacing JH-2 explosive with many new advanced energetic materials that have been reported that fulfil insensitive munitions requirements including IMX-101 and IMX-104 (Anniyappan et al. 2020)(K. E. Lee et al. 2010). A recent work by Dany Frem describes the entire manufacturing process for IMX-101 and IMX-104 under a common low-cost insensitive munition explosive program abbreviated as CLIMex(Frem 2023). This study highlights the importance and urgent need to replace conventional explosives such as JH-2 with novel explosives such as IMX-101 and IMX-104 in order to avoid the deadly and costly accidents of the past. These adaptations will reduce risks, increase safety, and increase operational effectiveness in regions where conventional munitions such as JH-2 are still widely used. By embracing this transition, continuous occurrence of accidental detonations will be significantly reduced making the whole world a safer place to live.

6. Conclusion

This research underscores the pivotal role that standard shaped charges play in evaluating munition safety parameters, essential to mitigate the tragic loss of lives and substantial financial damage caused by accidental detonations. The study's innovation lies in employing a compact 50mm standard shaped charge setup to effectively replicate the effects of 40mm grenades and medium-sized munitions. By strategically incorporating aluminum and steel buffer plates, the research adeptly assesses the safety characteristics of the JH-2 explosive and insensitive explosives. The meticulous selection of buffer plate materials, guided by rigorous AUTODYN simulations, attenuates the shaped charge jet's original energy output, yielding tailored configurations for subsequent safety analyses. These optimized setups facilitate comprehensive assessments of JH-2 explosive safety through empirical and computational means. The agreement between simulation outcomes and experimental results, confirmed by X-ray analysis and depth of penetration experiment, validates the approach's accuracy and underscores the effectiveness of simulation techniques. Moreover, the study highlights the profound influence of confinement conditions on explosive detonation probabilities, a key finding with implications for munition safety assessment. Important findings are listed as follows

1. The analysis of safety for JH-2 explosive exhibited inadequate performance, resulting in detonation across two trials, characterized by v^2d measurements of 68 $mm^3/\mu sec^2$.
2. During testing, the JH-2 explosive detonated when subjected to a 10mm steel cover, while it remained secure when surrounded by 20mm steel covers both in front and behind the explosive, against a shaped charge jet with a v^2d value of 37 $mm^3/\mu sec^2$

3. The empirical results, culminating in the detonation of the JH-2 explosive, found reinforcement through dedicated numerical simulations tailored for this specific explosive material.
4. Numerical simulation also confirmed the safety of insensitive munitions such as LX-17 and TATB under the same threat level encountered by JH-2 in this study.

Author's Contributions: Writing-original draft preparation, MS Awan.; supervision, funding acquisition, ZX Huang; Test technical support, X Zu and QQ Xiao.; conceptualization, ZX Huang and X Zu; methodology, MS Awan; software, MS Awan; validation, ZX Huang., X Zu and M Bin; writing—review and editing, X Zu and MS Awan

Editor: Marcílio Alves

References

Ahmed, M., and A. Q. Malik. 2017. "A Review of Works on Shaped Charges." *Engineering, Technology & Applied Science Research* 7 (5): 2098–2103. https://doi.org/10.48084/etasr.1532.

Anniyappan, M., M. B. Talawar, R. K. Sinha, and K. P.S. Murthy. 2020. "Review on Advanced Energetic Materials for Insensitive Munition Formulations." *Combustion, Explosion and Shock Waves* 56 (5): 495–519. https://doi.org/10.1134/S0010508220050019.

Arnold, W. and Rttenkoler, E. 2012. "'Shaped Charge Jet Initiation Phenomena of Plastic Bonded Explosives', Proceedings of the 2012 Insensitive Munitions & Energetic Materials Technology Symposium." In .

Arnold, Werner, and Ernst Rottenkolber. 2013. "High Explosive Initiation Behavior by Shaped Charge Jet Impacts." *Procedia Engineering* 58 (0): 184–93. https://doi.org/10.1016/j.proeng.2013.05.022.

AUTODYN 1998, Theory Manual, Revision 4.0. Century Dynamics Inc.

Baker, Ernest L., Arthur Daniels, Stanley Defisher, Nausheen Al-Shehab, Koon Wing Ng, Brian E. Fuchs, and Felix Cruz. 2015. "Development of a Small Shaped Charge Insensitive Munitions Threat Test." *Procedia Engineering* 103: 27–34. https://doi.org/10.1016/j.proeng.2015.04.005.

Baker, Ernest L., James Pham, Timothy Madsen, William Poulos, and Brian E. Fuchs. 2013. "Shaped Charge Jet Characterization and Initiation Test Configuration for IM Threat Testing." *Procedia Engineering* 58 (Im): 58–67. https://doi.org/10.1016/j.proeng.2013.05.009.

Daniels, Arthur, Stan Defisher, Greg Stunzenas, AL-SHEHAB Nausheen, and Ernest L Baker. 2017. "Development and Evaluation of Small Shaped Charge Jet Threats." *Problems of Mechatronics. Armament, Aviation, Safety Engineering* 8 (1): 23–38.

Davis, Robert J. Spear and Louise M. 1989. "An Australian Insensitive Munitions Policy, AD-A207950." Department of Defence, Defence Science and Technology Organisation, Materials Research Laboratory.

Downes, Devon, Amal Bouamoul, and Manouchehr N Ensan. 2014. "Numerical Simulation of the Shaped Charge." DEFENCE RESEARCH AND DEVELOPMENT CANADA VALCARTIER (QUEBEC) VALCARTIER Canada.

Elshenawy, Tamer, and Q M Li. 2013. "Influences of Target Strength and Confinement on the Penetration Depth of an Oil Well Perforator." *International Journal of Impact Engineering* 54: 130–37.

Frem, Dany. 2023. "A Review on IMX-101 and IMX-104 Melt-Cast Explosives: Insensitive Formulations for the Next-Generation Munition Systems." *Propellants, Explosives, Pyrotechnics* 48 (1): e202100312.

Fuchs, Brian. 2018. "Review and Update of STANAG 4526 Shaped Charge Jet, Munitions Test Procedure." San Diego CA: International Explosives Safety Symposium & Exposition.

Gilbert, Lee N. 1991. "Technical Evaluation Report, AD-A255698." In *Conference Proceedings 511*. Advisory Group for Aerospace Research & Development.

Hayles, Danny R. 2005. "How Safe Should Our Weapons Be." AIR UNIV MAXWELL AFB AL.

Held, Manfred. 1987. "Discussion of the Experimental Findings from the Initiation of Covered, but Unconfined High Explosive Charges with Shaped Charge Jets." *Propellants, Explosives, Pyrotechnics* 12 (5): 167–74.

Lee, E L, H C Hornig, and J W Kury. 1968. “Adiabatic Expansion of High Explosive Detonation Products.” Univ. of California Radiation Lab. at Livermore, Livermore, CA (United States).

Lee, Edward L, and Craig M Tarver. 1980. “Phenomenological Model of Shock Initiation in Heterogeneous Explosives.” *The Physics of Fluids* 23 (12): 2362–72.

Lee, K E, W A Balas-Hummers, A R Di Stasio, C H Patel, J Samuels, B D Roos, and Virgil Fung. 2010. “Qualification Testing of the Insensitive TNT Replacement Explosive IMX-101.” In *Insensitive Munitions and Energetic Materials Technology Symposium*, 1–13.

Li, Xiang-dong, Yan-shi Yang, and Sheng-tao Lv. 2014. “A Numerical Study on the Disturbance of Explosive Reactive Armors to Jet Penetration.” *Defence Technology* 10 (1): 66–75.

Liu, Yakun, Jianping Yin, and Zhijun Wang. 2019. “Study on the Overdriven Detonation Wave Propagation in Double-Layer Shaped Charge.” *Physics of Fluids* 31 (9): 92110.

Liu, Yakun, Jianping Yin, Zhijun Wang, Xuepeng Zhang, and Guangjian Bi. 2020. “The EFP Formation and Penetration Capability of Double-Layer Shaped Charge with Wave Shaper.” *Materials* 13 (20): 4519.

NATO. 2010. “Guidance on the Assessment and Development of Insensitive Munitions, Allied Ordnance Publication 39.” NATO.

Peron, P.F. 2004. “‘MSIAC Workshop on IM Technology Gaps’, Proceedings of the 2012 Insensitive Munitions & Energetic Materials Technology Symposium.”

Scherpelz, R I, R J Traub, J G Droppo, and M A Parkhurst. 2000. “Depleted Uranium Exposures to Personnel Following the Camp Doha Fire, Kuwait, July 1991.” *Report Prepared for the US Army Center for Health Promotion and Preventive Medicine by Pacific Northwest National Laboratory, Richland, WA*.

Selivanov, V. V., S. V. Fedorov, A. V. Babkin, and I. A. Bolotina. 2021 “Using Shaped Charges with a ‘Magnetic Cut-off’ for Testing Anti-Meteoroid Shields.” *Acta Astronautica* 180 (November 2020): 170–75. https://doi.org/10.1016/j.actaastro.2020.12.026.

Shekhar, Himanshu. 2012. “Theoretical Modelling of Shaped Charges in the Last Two Decades (1990-2010): A Review.” *Central European Journal of Energetic Materials* 9 (2): 155–85.

Souers, P Clark, Raul Garza, and Peter Vitello. 2002. “Ignition & Growth and JWL++ Detonation Models in Coarse Zones.” *Propellants, Explosives, Pyrotechnics: An International Journal Dealing with Scientific and Technological Aspects of Energetic Materials* 27 (2): 62–71.

Spasskiy, Nikolai. 2001. *XXI Century Encyclopedia, Russia’s Arms and Technologies, Volume II: Rocket and Artillery Armament of Ground Forces*. Moscow: The Publication House, “Arms and Technologies.”Xiao, Qiang-Qiang, Zheng-Xiang Huang, Xu-Dong Zu, and Xin Jia. 2016. “Influence of Drift Velocity and Distance between Jet Particles on the Penetration Depth of Shaped Charges.” Propellants, Explosives, Pyrotechnics 41 (1): 76–83.

Xu, Wenlong, Cheng Wang, and Dongping Chen. 2019. “Formation of a Bore-Center Annular Shaped Charge and Its Penetration into Steel Targets.” *International Journal of Impact Engineering* 127: 122–34.

Zhang, Quan, Jiong Wang, Shan Guo, Weili Gong, Longfei Feng, Haosen Wang, Can Ming, and Zimin Ma. 2021. “Shaped Charge Hydraulic Blasting: An Environmental, Safe, and Economical Method of Directional Roof Cutting.” *Geofluids* 2021. https://doi.org/10.1155/2021/5511081.

Zhang, Xian-feng, Zheng-xiang Huang, and Liang Qiao. 2011. “Detonation Wave Propagation in Double-layer Cylindrical High Explosive Charges.” *Propellants, Explosives, Pyrotechnics* 36 (3): 210–18.